Angewandte Chemie
Eine Zeitschrift der Gesellschaft Deutscher Chemiker

Supporting Information

In Situ Growth and Characterization of Metal Oxide Nanoparticles Within Polyelectrolyte Membranes

John Landers[+], *Jonathan Colon-Ortiz*[+], *Kenneth Zong, Anandarup Goswami, Tewodros Asefa, Aleksey Vishnyakov, and Alexander V. Neimark**

anie_201606178_sm_miscellaneous_information.pdf

A. MATERIALS AND EXPERIMENTAL METHODS

A.I. Materials:

Nafion-117 ionomer membrane with an equivalent weight of 1100 g/SO_3H was purchased from Ion Power, Inc. Salt reagents zinc nitrate (98%), cobalt(II) nitrate (98%), iron(III) nitrate (98%), nickel(II) nitrate(98.5%), magnesium(II) nitrate (98%), and sodium hydroxide (>97%) were purchased from Sigma-Aldrich.

A. II. Membrane Preparation:

For standard MONP-Nafion composite films, Nafion membranes were cut into 0.5 x 0.5 inch films about 200 μm in thickness, and soaked in 10 mL of an aqueous 0.05 M metal salt solution for 24 h at room temperature (RT). The membranes were then removed, rinsed in DI and placed in 0.5 M aqueous NaOH solution for a period of 6 h at 60 °C to promote hydrolysis towards the metal hydroxide. After 6 h, the films are removed from the NaOH solution and rinsed briefly in DI. The films are then placed in an empty vial for 24 h at 100 °C. The above procedure was repeated for the synthesis of the bulk metal oxide nanoparticles without the membrane by mixing equal volumes of 0.05 M metal salt with 0.5 M aqueous NaOH solution for 6 h at 60 °C. The particles are then filtered and rinsed and placed in the furnace for 24 h at 100 °C to induce oxidation of the MONP.

A. III. Characterization:

Scanning electron microscopy: Cleaved cross sections of the membranes were obtained by dipping them in liquid nitrogen for 30 sec prior to cutting. TEM was performed using a JEOL 1200EX transmission electron microscope. About 10 mg of metal-oxide powder was added to 1 mL of ethanol and sonicated for 5 minutes. After sonication, one drop of ethanol/MONP solution was added to a TEM copper grid (FORMVAR, 400 Mesh, carbon film coated copper grid, or FCF400-Cu from Electron Microscopy Sciences) and was left to air-dry. Analysis on TEM was done afterwards. SEM was performed with the Zeiss Sigma Field Emission SEM with Oxford EDS. X-ray diffraction patterns were obtained by using a wide angle Philips XPert system. The same procedure was used for the HAADF-STEM images, albeit lacey carbon TEM grids were employed and was performed using a Nion UltraStem equipped with an aberration corrector,

which allows us to obtain spatial resolution down to ~1 Å at an operating voltage of 60 kV. The condenser lens system was set to produce an illumination probe semi-angle of 35 mrad and a beam current of ~10–20 pA.

WAXRD patterns were obtained by the Philips XPert system. For the XRD analysis, a baseline correction was applied to each pattern, limited to the range involving the three primary peaks. Baseline corrections were applied at the base of each peak. Absorption and transmission measurements were performed using a Photonics CCD Array UV-vis spectrometer

A large broad peak at low angles, spanning several tens of angles can be seen that is attributed to instrumental effects. At angles of 2Θ between 25 to 55 degrees, the observed broadening is attributed to the amorphous polymer host. These factors somewhat affect the heights of the 3 primary peaks corresponding to the dominant surface planes of zinc oxide. In addition, broadening of individual peaks is also observed throughout the XRD pattern arising from a convoluted number of factors such as lattice strain, particle size, orientation, and possible dislocations and stacking faults.[1]

Absorption and transmission measurements were performed using a Photonics CCD Array UV-vis spectrometer and using the model of Pesika et al.[2] Briefly, the authors use an effective mass model for spherical particles with a Coulomb interaction term[3] where the bandgap E* [eV] can be approximated by:

$$E* \cong E_g^{Bulk} + \frac{\hbar^2\pi^2}{2er^2} - \left(\frac{1}{m_e m_0} + \frac{1}{m_h m_0}\right) - \left(\frac{1.8e}{4\pi\varepsilon\varepsilon_0 r}\right) \quad (1)$$

Where E_g^{Bulk} is the bulk bandgap, r is the particle radius, m_e is the effective mass of the electron, m_h is the effective mass of the holes, m_0 is the free electron mass, ε is the relative permittivity, ε_0 is the permittivity of free space, ħ is Plank's constant, and e is the charge of the electron. Parameters for ZnO are given by: E_g^{Bulk} = 3.2 eV, ε = 8.5, m_e = 0.26, and m_h = 0.59.

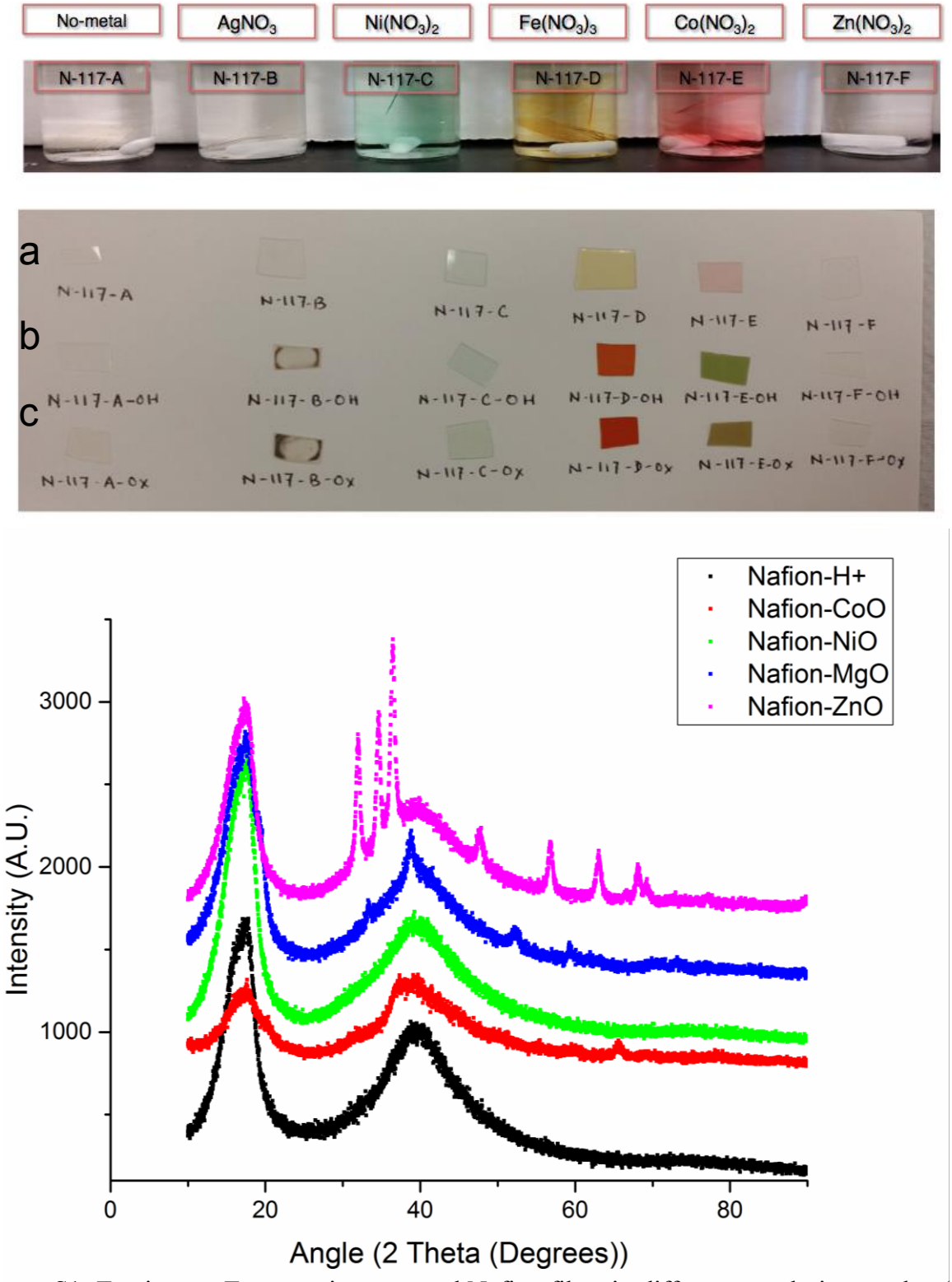

Figure S1: Top image: Top row: impregnated Nafion films in different metal nitrate salts. (a) Nafion membranes after ion exchange step. (b) Nafion membranes after hydrolysis step. (c) Nafion membranes after condensation step. Suffix –OH and –OX stand for metal hydroxide and metal oxide, respectively. Bottom Graph: XRD pattern of different metal oxides synthesized in situ.

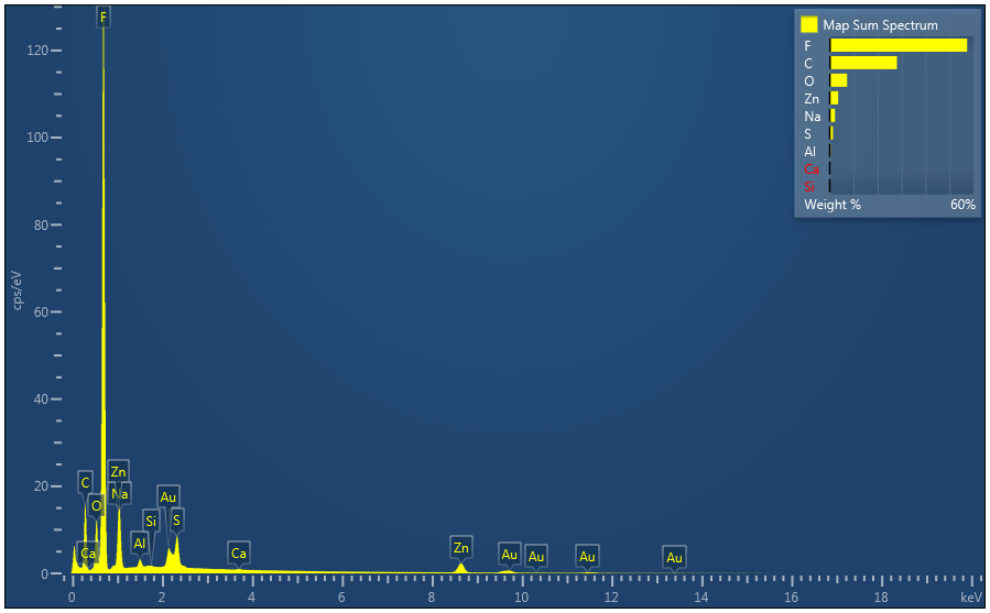

Figure S2: Electron diffraction spectroscopy (EDS) of a Nafion cross section displayed in Figure 2c in the manuscript.

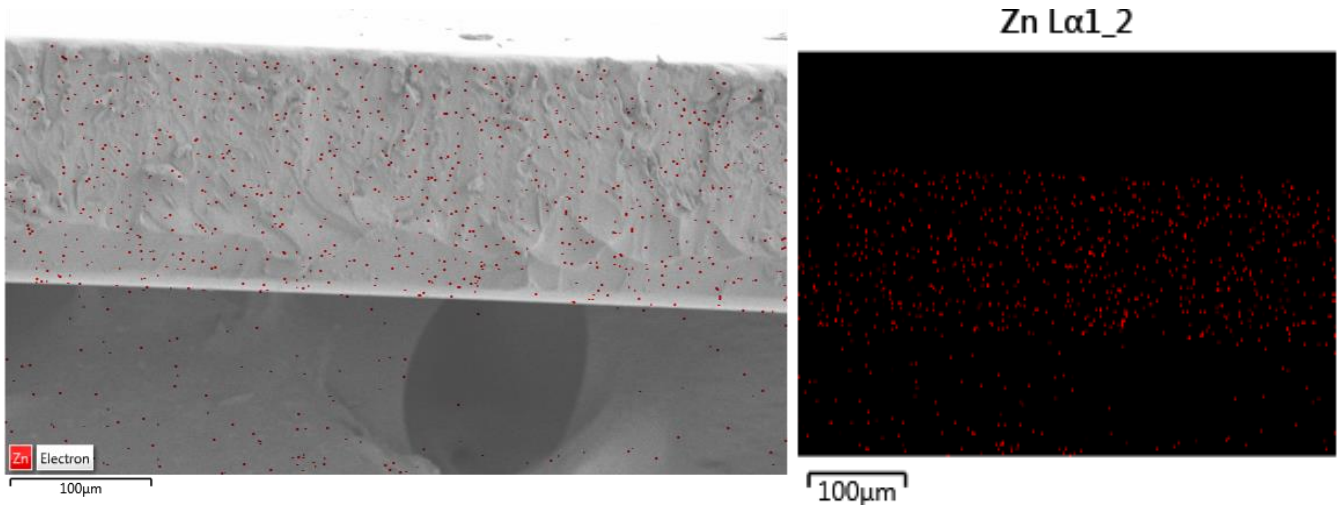

Figure S3: SEM/EDX of the ZnO/Nafion membrane edge uncut. (Left) The edges lack the high concentration of Zn that results from deformation upon cutting. (Right) EDX mapping only. Zinc seen on the carbon tape arises from ZnO particles on the surface of the ZnO/Nafion composite that were transferred during specimen preparation.

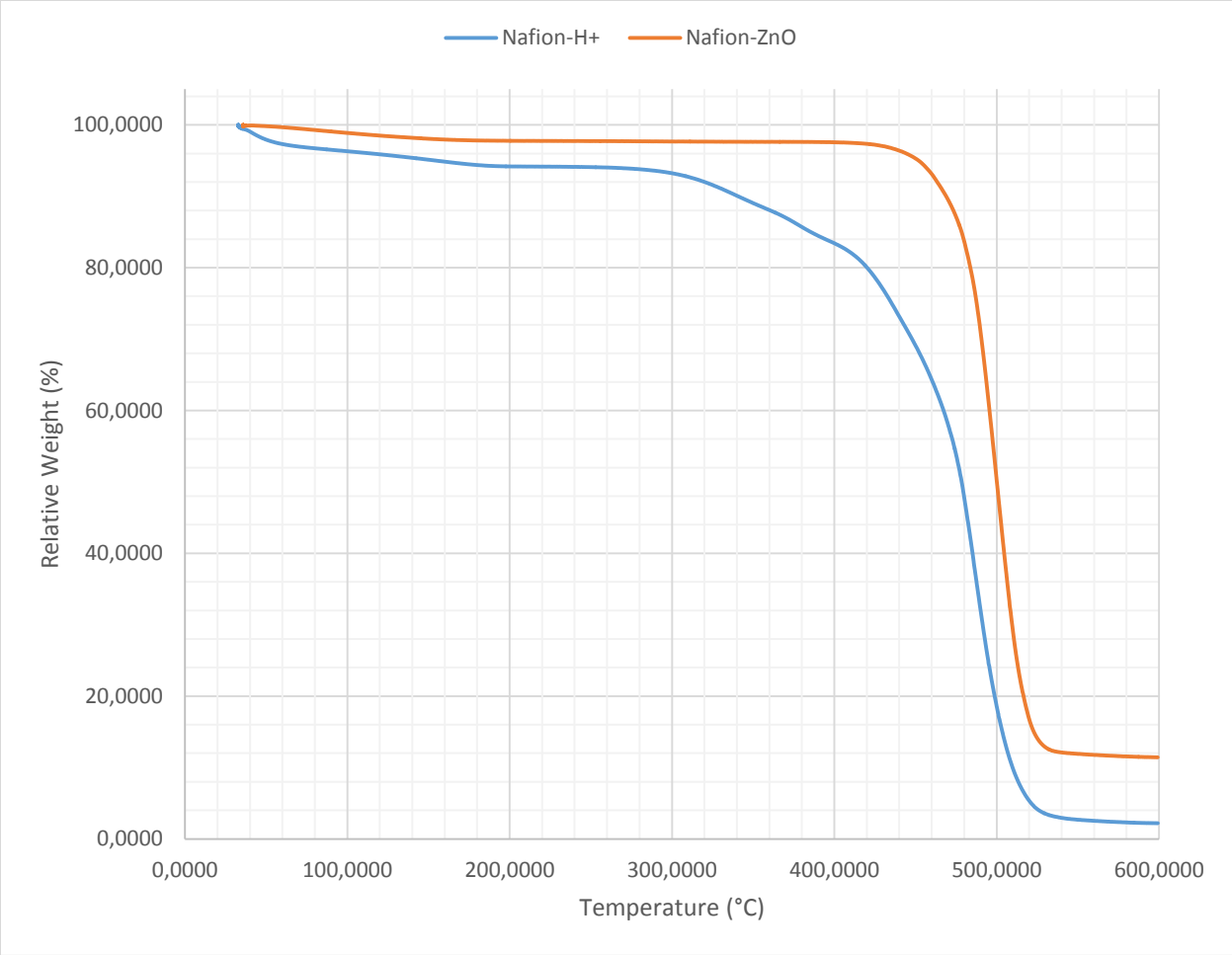

Figure S4: Thermogravimetric analysis (TGA) traces of the ZnO-Nafion films grown from a 0.05 M $Zn(NO_3)_2$ solution.

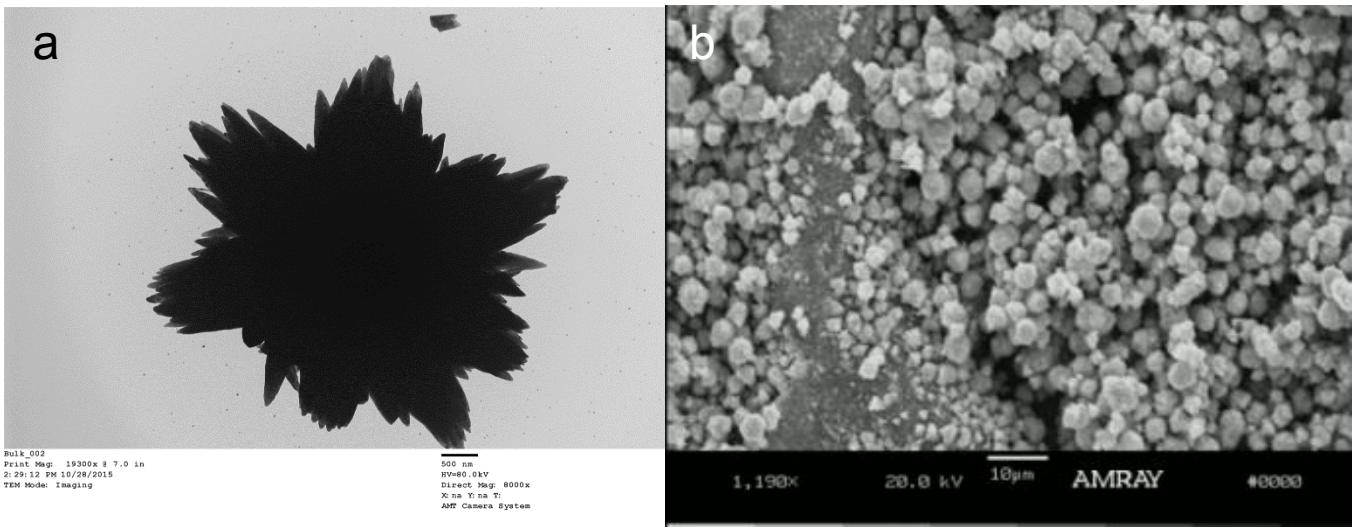

Figure S5: (a) TEM image of zinc oxide nanoparticle prepared in bulk and without the Nafion-117 host membrane. (b) SEM image of the bulk nanoparticles.

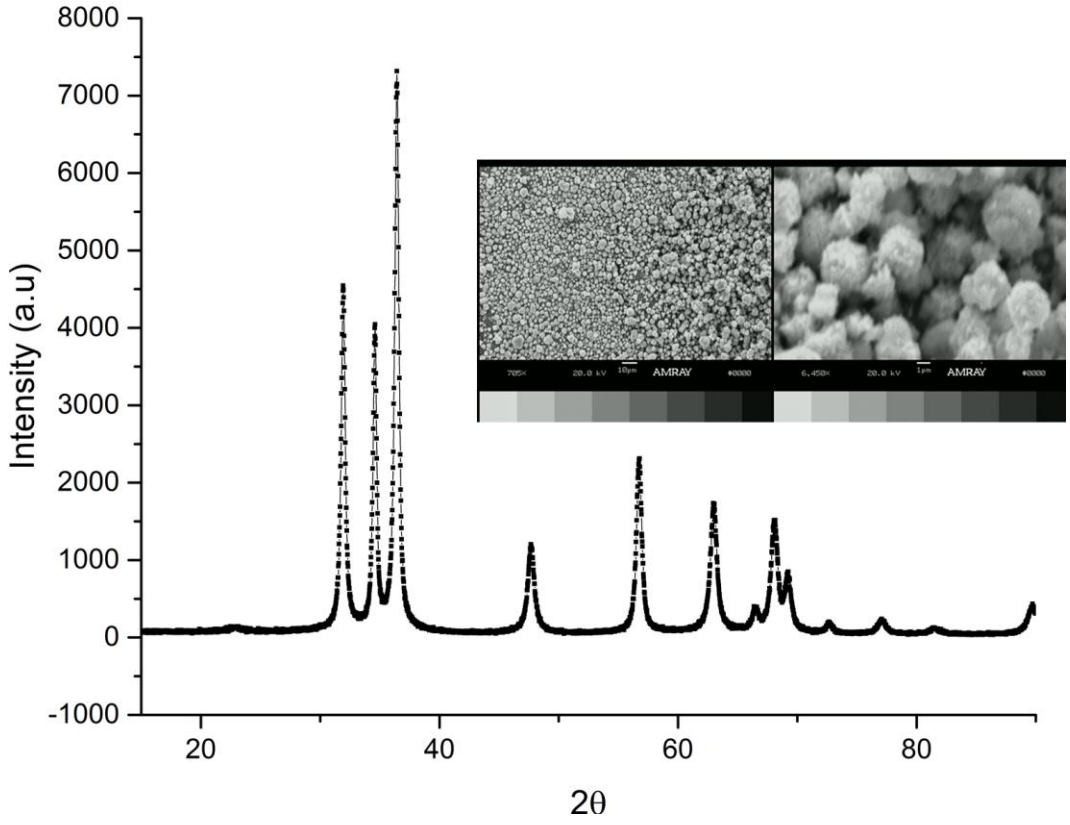

Figure S6: XRD of the bulk zinc oxide prepared without the Nafion-117 membrane. Insets shows the SEM images of the zinc oxide powder.

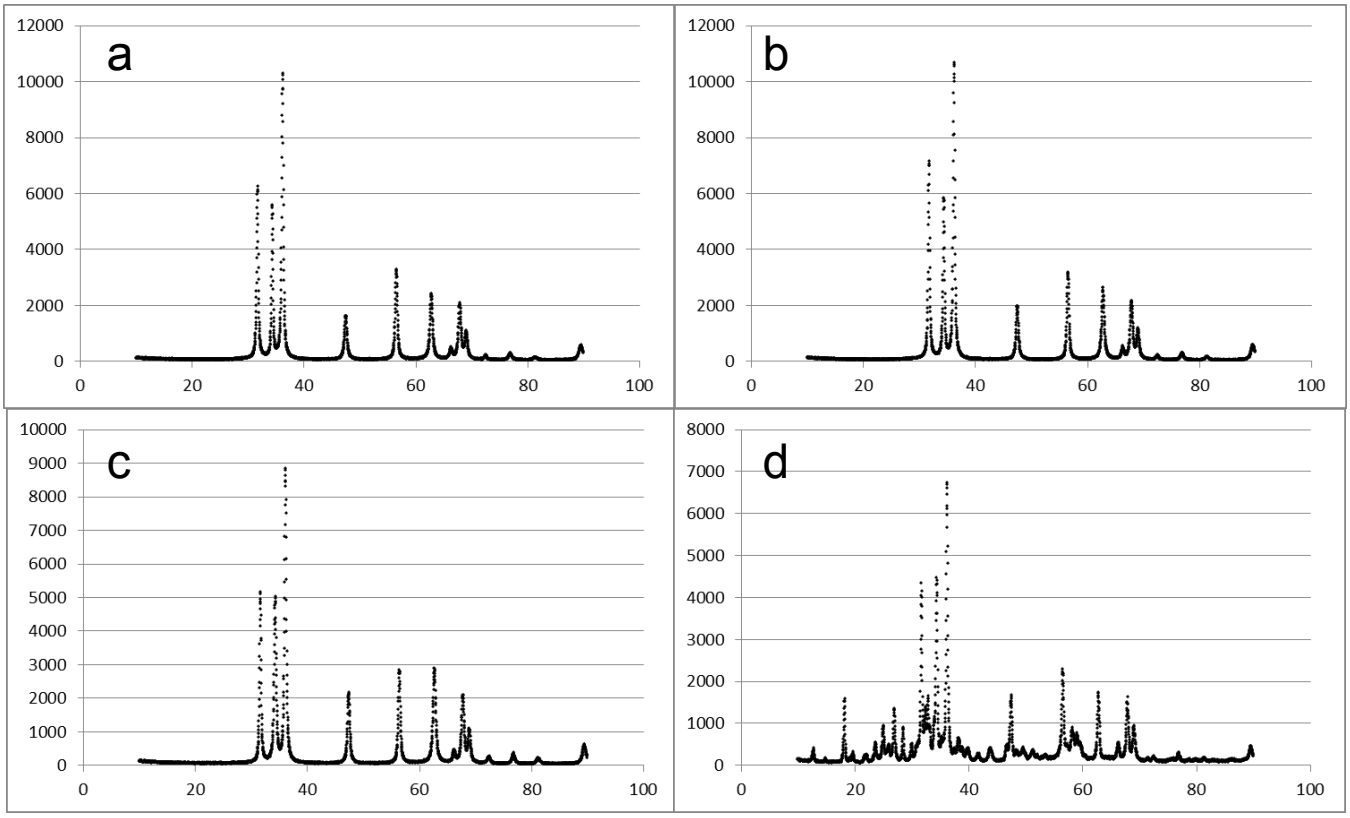

Figure S7. Bulk synthesis of ZnO with 2-propoanol. (a) 20% (b) 40% (c) 60% and (d) 80%. Y-axis is intensity (a.u.) and X-axis is 2Θ.

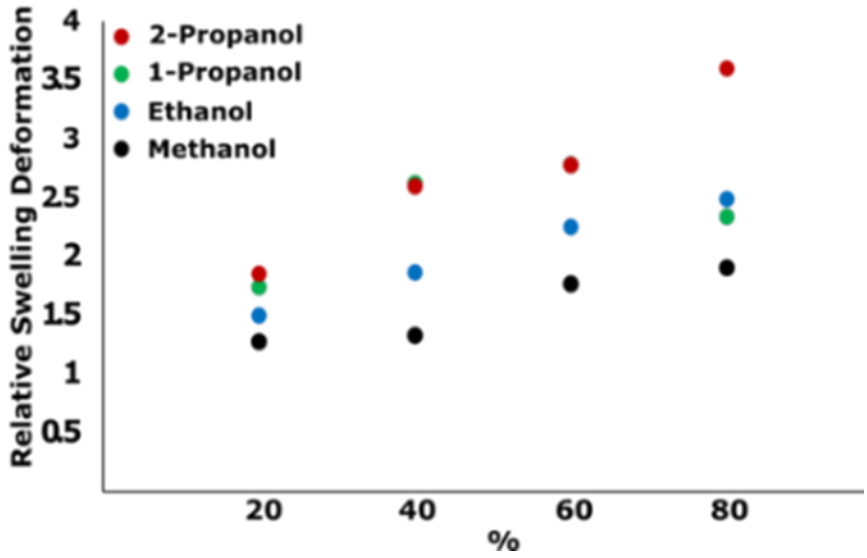

Figure S8: Swelling behavior of Nafion-117 film prepared in different alcohols at different concentrations. Film dimensions were measured after the impregnation of the metal salt.

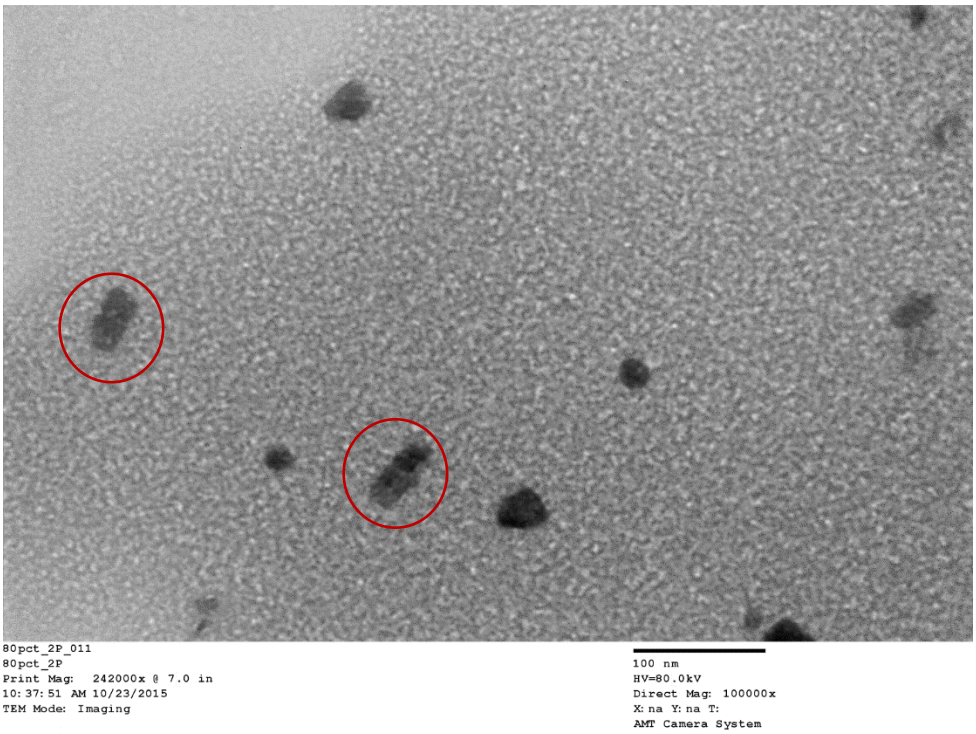

Figure S9: TEM images showing the twinning of two particles grown in adjacent hydrophilic domains in Nafion 117 membrane. Films were prepared in a 80% 2-propanol/water binary mixture.

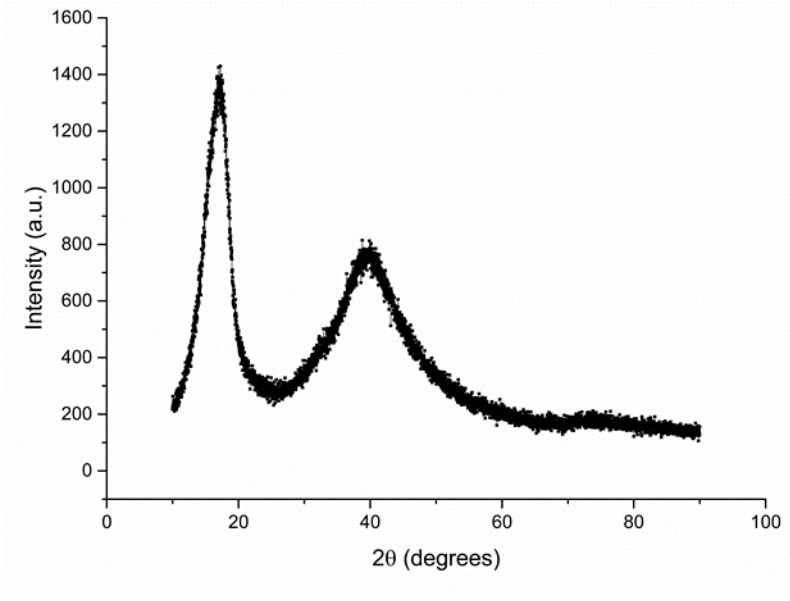

Figure S10: XRD pattern of MONP-Nafion composites synthesized without the inclusion of water.

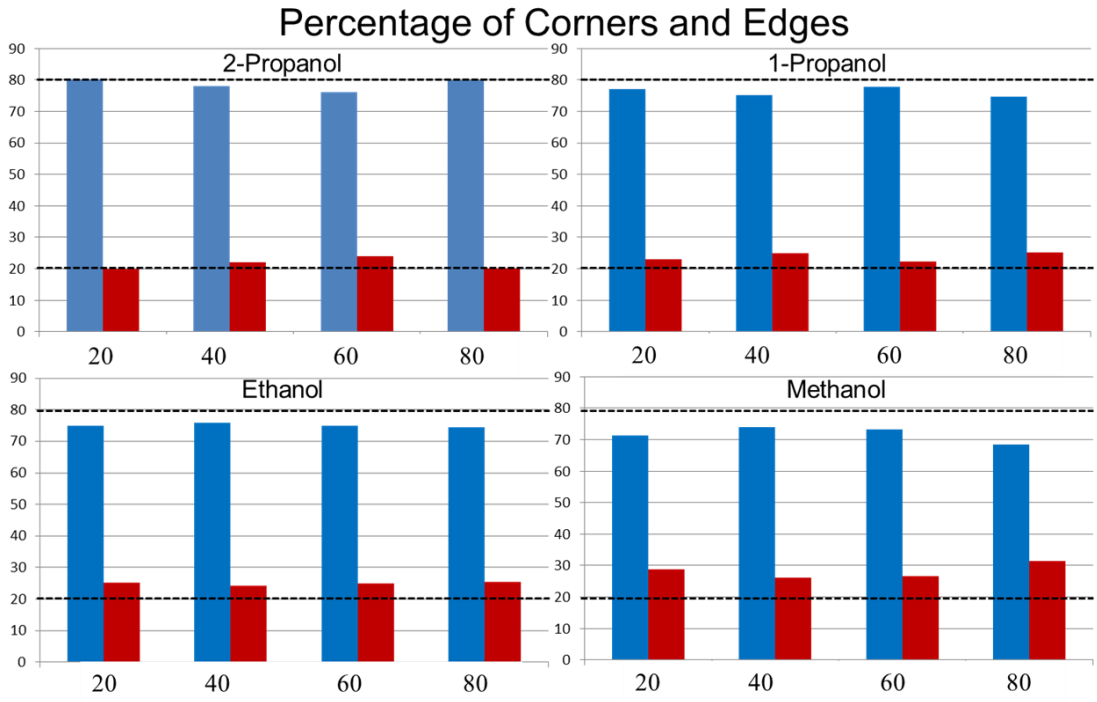

Figure S11: XRD analysis of films prepared with different alcohols at different concentrations. Blue column represents the accumulated peak intensities for the {100}, {002} and {100} planes. Red column represents the peak intensities for the {102}, {110}, {103} and {112} planes. The top dotted line marks the 80% mark for the cumulative portion while the bottom dotted line marks 20%.

B. SIMULATIONS METHODS:

Dissipative particle dynamics (DPD) simulations were performed in accordance with procedures followed in ref [4]

B. I. Relative volumes of the beads

Table S1.

Bead	**W**	**C**	**E**	**S**	**S□**
Fragment	$(H_2O)_{4.5}$	$(-CF_2-)_4$	-O-CF(CF3)-	$(-CF_2-)_2SO_3K$	$(-CF_2-)_2SO_3^-$

			CF2-O		
Σr_i [(a)]	4.14	4.04	3.67		
Representative compound [(b)]	H_2O	$H(CF_2)_4H$	$CF_3OCFOCF_2H$	$H(CF_2)_2SO_3K$	$H(CF_2)_2SO_3^-$
V_{COSMO}	29.1	141.1	112.7	124.2	140.7
Effective volume, Å^3	134.5	131.3	117.1	119.3	136.5

(a) sum of volume parameters r_i for the functional group forming the fragment

(b) molecule, for which the COSMO volume was calculated using PQS ab-initio; correspondingly V_{COSMO} is the volume of the molecule, rather than the bead volume

B. II. Details of MD simulations for DPD parameter fitting

The simulation procedures were similar to those employed in refs. [5] We used MDynaMix [6] software package. In the initial configuration, molecules were arranged in a lattice order at a low density of 0.005 g/cm^3. The system was then gradually contracted in a series of constant-temperature MD simulations at T = 303K maintained by a simple velocity scaling. After the density of 1.0g/cm^3 (aqueous solutions) or 1.7 g/cm^3 (perfluorohexadecane) was achieved, the simulation proceeded at a constant pressure P = 1atm . T and P were maintained by the Nose-Hoover thermostat. [7] System equilibration was performed for 200 ps followed by additional 10 to 1 ns MD simulation, over which the system configuration was periodically saved to disc for analysis. The distribution of distances between the beads in DPD simulations were fitted to the distances between the centers of mass of the corresponding fragments (see Table 1 in

the main text and Table S1). In order to maintain symmetry in Nafion model, we assumed that some fluorocarbon groups were divided between the two neighboring beads. In particular, the location of bead C1 from the MD trajectories of the Nafion fragment shown in Figure S1(a) was calculated as

$$\mathbf{r}_{C1} = (\mathbf{r}_3 * M_{CF} + \mathbf{r}_2 * M_{CF2} + \mathbf{r}_4 * M_{CF2} + 0.5 * \mathbf{r}_1 * M_{CF2} + 0.5 * \mathbf{r}_5 * M_{CF2}) / (M_{CF} + 4 * M_{CF2})$$

The indexes of fluorocarbon groups are also shown in the Figure.

(a)

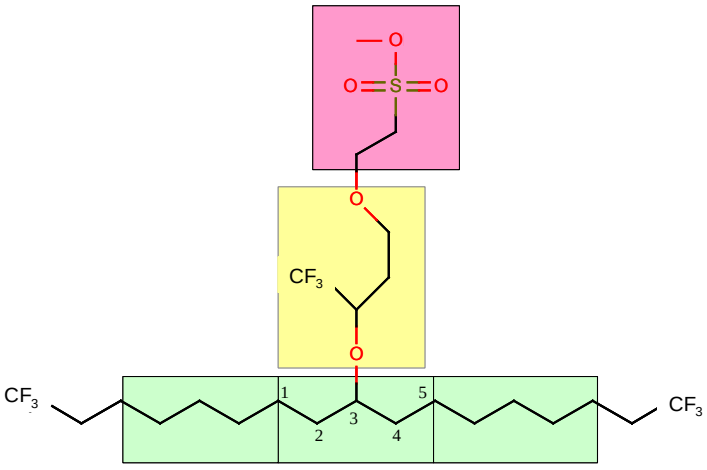

(b)

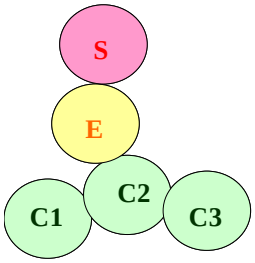

(c)

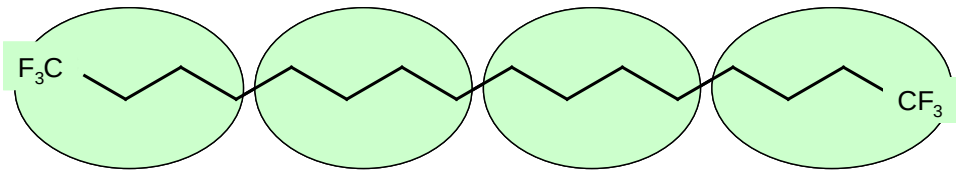

Figure S12. (a) Nafion fragment modeled in aqueous solution by molecular dynamics in order to obtain distribution of distances between the bead centers (b) coarse-grained model of Nafion fragment simulated by DPD (3) molecular and coarse-grained models of perfluorohexadecane.

B. III. Details of DPD simulations.

Nafion was presented by oligomers each containing 20 monomers. Bead density $\rho * R_c^3$ in the system was set to 3, a common choice for aqueous solutions. The random force, which accounts for thermal fluctuations, is taken proportional to the conservative force that is also acting along the vector between the bead centers: $\boldsymbol{F}_{ij}^{(R)}(r_{ij}) = \sigma w^R r_{ij} \theta_{ij}(t) \mathbf{r}_{ij}$, where $\theta_{ij}(t)$ is a randomly fluctuating in time variable with Gaussian statistics. The drag force is velocity-dependent: $\boldsymbol{F}_{ij}^{(D)}(\mathbf{r}_{ij}, \mathbf{v}_{ij}) = -\gamma w^D(r_{ij}) (\mathbf{r}_{ij} * \mathbf{v}_{ij})$, where, $\mathbf{v}_{ij} = \mathbf{v}_j - \mathbf{v}_i$, $\mathbf{v}_i$ and $\mathbf{v}_j$ are the current velocities of the particles. We assume the common relationship between the drag and random force parameters $w^D(r) = [w^R(r)]^2$. σ and γ are parameters that determine the level of energy fluctuation and dissipation; they are related as and $\sigma^2 = 2\gamma kT$ that allows to maintain constant temperature in the course of simulation. We assumed $\gamma = 4.5$, a common value fitted to the diffusion coefficient of water. In the initial configuration, all beads were assigned random locations in the box. Starting from this random configuration, we performed a steepest descent energy minimization taking in account only harmonic bond and short-range conservative forces. The minimization was followed by 10000 step preliminary MD simulation ($\gamma = 0$, no drag or random forces) at temperature fixed by velocity scaling on each step. DPD simulations started from the final configuration obtained in that preliminary MD run. In-house DPD program was used.

B. III.A. Simulations of Nafion fragments employed in forcefield fitting.

The systems exactly mimicked the MD simulations (Tabke S2). Simulations were 150000 DPD steps long, time step in reduced time units was $0.02(m_W R_c^2/kT)^{1/2}$. First 50000 steps were discarded. After that the coordinates of all beads except solvent beads were dumped to disk every 100 steps. The distributions of intramolecular distances and angles were calculated from this trajectory. In first simulations, we used reasonable bond parameters approximately evaluated from average distances and dispersions obtained in MD simulations. Then, the bonds were optimized from one simulations to another in order to improve the agreement with the MD results similarly to ref [8]

B. III.B. Simulations of hydrated Nafion

Nafion was presented by oligomers each containing 20 monomers. Simulations were conducted in cubic boxes of $30R_c$ (22.3nm) in size, the total number of beads was around 81000 in each simulations. The total numbers of bneads of each type is given in the table at the botoom of this section. On the minimization and preliminary scaled-velocity MD stages, all beads were uncharged. Before DPD simulations started, S beads were converted to S- (at low hydration, the beads for conversion were chosen randomly), and randomly chosen W beads were converted to M+ beads, according to the targeted system composition. The total number of DPD steps was 800000 in each simulation. The initial configuration was created by placing all beads at random coordinates within the simulation box. Then the energy was minimized using a primitive steepest descent algorithm, which lead to a segregated system with small hydrophilic clusters of several W, S and M beads. The minimization was followed by 10000 step preliminary MD simulation (γ = 0, no drag or random forces) at temperature fixed by velocity scaling on each step. DPD

simulations started from the final configuration obtained in that preliminary MD run. DPD simulations were started from these configurations. First 200000 DPD steps were performed with no long-range correction (electrostatic interactions were cut off at $5R_c$), and after that, Ewald summation was turned on to account for the long-range electrostatics. The structural evolution was characterized using the number of overlapping pairs of mobile (W and M+) beads as a criterion. The initial portions of each trajectory characterized by a persistent upward trend (about 400000 steps) were discarded. Over the last 400000 steps, the system configuration was dumped to disk every 1000 steps. In so doing, we collected 400 configurations for structural analysis and the calculation s of chemical potentials of water via Widom insertions.

Table S2. Numbers of beads of different types in each simulation. The number of M^+ (hydrated counterion) beads equals the number of S^- beads. There were no W beads in all simulations for λ=2.24

λ =		2.2			4.5			6.8	
PEW	S-	S	C	S-	W	C	S-	W	C
945	11172	6284	52371	15511	3447	46532	17153	12388	51459
1145	9191	5170	57447	13018	2893	52071	14155	10223	56621
1345	7807	4392	60994	11215	2492	56077	12050	8702	60248
1745	6000	3375	65625	8783	1952	61482	9287	6707	65006

	9.0			13.5			18.0	
S-	W	C	S-	W	C	S-	W	C
15511	18957	46532	13018	28929	39054	11215	36138	33646
13018	15911	52071	11215	24923	44862	9851	31743	39405
11215	13708	56077	9851	21892	49257	8783	28301	43916
8783	10735	61482	7924	17609	55467	7218	23257	50525

III. C. Electrostatic interactions: comparison between smeared and point charges.

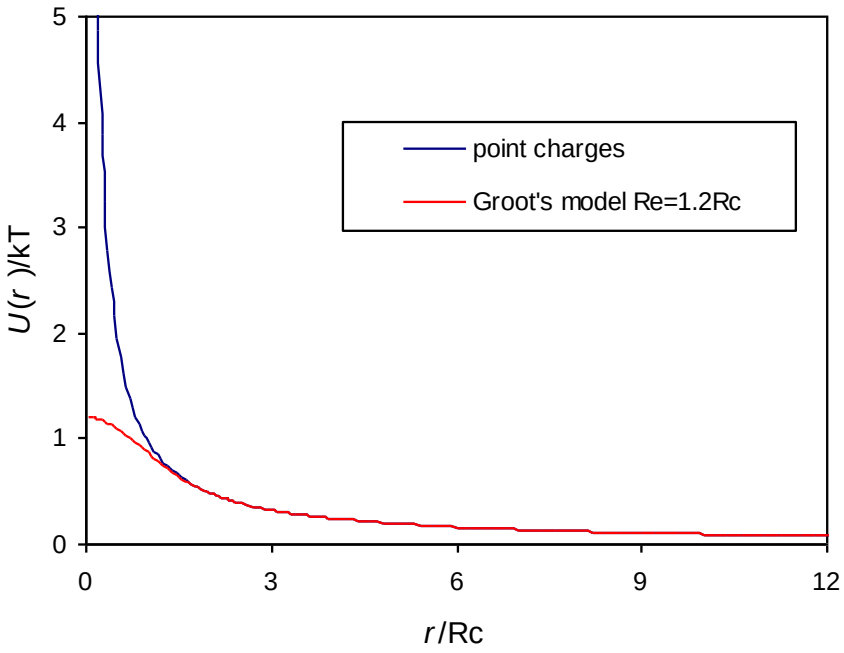

Figure S13. Comparison of electrostatic potential between two +*e* point charges and linearly smeared charges with smearing radius of R_e=1.2R_c in a dielectric medium of □□= 78, which corresponds to .water at room temperature.

B. IV. Water sorption and diffusion in hydrated Nafion

Table S3. Main results.

λ =	9			13.5			18		
PEW	m_W/m_{pol}, %	ϕ_W, %	D_W/D_{pure}	m_W/m_{pol}, %	ϕ_W, %	D_W/D_{pure}	m_W/m_{pol}, %	ϕ_W, %	D_W/D_{pure}
945	16.5	28.6	0.12	24.7	37.5	0.11	32.9	44.4	0.04
1145	13.7	25.0	0.014	20.5	33.3	0.009	27.4	40.0	0.002
1345	11.7	22.2	0.0009	17.6	30.0	0.0002	23.4	36.4	0
1745	9.1	18.2	0	13.6	25.0	0	18.2	30.8	0

λ =	2.24			4.5			6.75		
PEW	m_W/m_{pol}, %	ϕ_W, %	D_W/D_{pure}	m_W/m_{pol}, %	ϕ_W, %	D_W/D_{pure}	m_W/m_{pol}, %	ϕ_W, %	D_W/D_{pure}
945	4.1	9.1	0.001	8.2	16.7	0.011	12.3	23.1	0.062
1145	3.4	7.7	0	6.8	14.3	0.0029	10.3	20.0	0.0087
1345	2.9	6.6	0	5.9	12.5	0.0002	8.8	17.6	0.0019
1745	2.3	5.2	0	4.5	10.0	0.0001	6.8	14.3	0.0006

m_W/m_{pol} are calculated assuming K^+ as cation

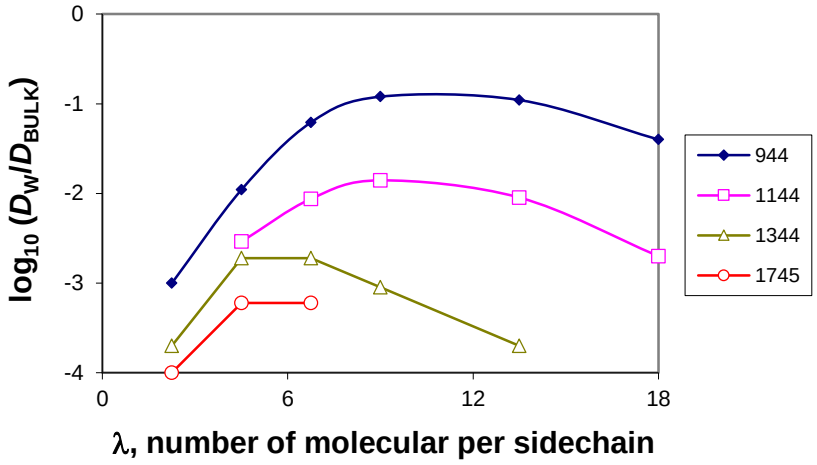

Figure S14. Self-diffusion coefficient of water in hydrated Nafion reduced to the diffusion coefficient of pure water for polymers of hydration level λ.

C. LITERATURE REVIEW OF WORKS DEMONSTRATING THE IN SITU GROWTH OF AN INORGANIC PHASE WITHIN NAFION AND RELATED POLYMERS

First Author	Inorganic Phase	Comments	Precursor	Recommended Application	
Ai	Pt np			H2O2 sensor	[9]
Alberti				PEMFC	[10]
Amiinu	Silica			PEMFC	[11]
Amjadi	TiO_2		Tetrabutylortotitanate	PEMFC	[12]
Amjadi	SiO_2			PEMFC	
Babu	PbS			Quantum dots	[13]
Baradie	SiO_2		Tetraethoxysilane (TEOS)	PEMFC	[14]
Cele		Review Paper		PEMFC	[15]
Chalkova*	ZrO_2, SiO_2			PEMFC	
Chaundhury	SiO_2	Studied the IEC, water upatake and ion exchange isotherms of Na+ & Cs+ and Na+ & Ba2+ binary systems	Tetraethoxysilane (TEOS)		[16]
Chen	SiO_2		Tetraethylorthosilicate	PEMFC	[17]
Chen	Zeolite Beta	Hydrothermal crystalization		DMFC	[18]
Chi	ZnO nanorods	Grown ZnO rods first, then cast Nafion, then etched away ZnO.		PEMFC	[19]
Choi	MWNT/ZnO		Tris(2,2 '-bipyridyl) ruthenium(II)	Chemiluminescence sensor	[20]
Choi	ZrO_2	Proton transport properties		PEMFC	[21]
Choi*		Review		DMFC	[22]
Chowdhury		POM filtration		Filtration membranes	[23]
Colicchio	SPEEK/PWA			DMFC	[24]
Cui	Chitosan/ heteropolyacid			DMFC	[25]
Daiko	TiO_2/SiO_2		$Si(OC_2H_5)_4$ and $Ti(OC_4H_9)_4$		[26]

Daiko		Hygroscopic oxides	$Si(OC_2H_5)_4$ and $Ti(OC_4H_9)_4$	DMFC	[27]
Daiko	phenylsilsesquioxane	Nafion/PDDACl			[28]
Damay	SiO_2, ZrP	H_3PO_4 , $H_3PW_{12}O_{40}$ Transport properties		PEFC	[29]
Deng	SiO_2		Tetraethoxysilane (TEOS)		[30]
Deng	SiO_2		Tetraethoxysilane (TEOS) & diethoxydimethylsilane (DEDMS)		[31]
Deng	SiO_2	SAXS studies			[32]
Deng	SiO_2	Fluorescence probe investigations			[33]
Deng	SiO_2				[34]
Deng	SiO_2	TGA studies	Tetraethoxysilane & diethoxydimethylsilane		[35]
Doyle***	SWNT/Fe_2O_3	Redox and oxygen evolution studies		Redox	[36]
Dresch	SiO_2	SAXS/Neutron; prepared in different solvents		PEMFC	[37]
Dupuis		Review		PEMFC	[38]
Hill	ZrP	disulfonated poly(arylene ether sulfone)		DMFC	[39]
Huang	Pt			Non-enzymatic glucose sensing	[40]
Ingle (2014)	Pt nanorods	$Pt(NH_3)(4)(NO_2)(2)$		Catalysts for electrochemical devices	[41]
Jalani	ZrO_2, SiO_2, TiO_2			High Temp. PEMFC	[42]
Jiang	SiO_2		Tetraethylorthosilicate (TEOS)	DMFC	[43]

Jian-hua	TiO_2		Ti $(OC_4H_9)_4$	PEMFC	[44]
Jung	SiO_2		Tetraethylorthosilicate (TEOS)	DMFC	[45]
Kang	Strontium hydroxide			DMFC	[46]
Ke	SiO_2				[47]
Ke	SiO_2	Particle size			[48]
Kim	Fluoroalkysilane			Fuel cell operations tests	[49]
Kim	SiO_2				[50]
Kim	Alumina			PEMFC	[51]
Kim	Pd			DMFC	[52]
Kim	SiO_2	Proton conductivity and MeOH permeation	Tetraethylorthosilicate (TEOS)		[53]
Klein	SiO_2	Review		PEM	[54]
Klein		Review		PEM/DMFC	
Korin		Review		Fuel Cells	[55]
Kumar	Au	Anion exchange	$HAuCl_4$		[56]
Kumar	Ag	Poly(perfluorosulfonic) acid membrane			[57]
Kumar	Pt	Anion exchange membranes	$PtCl6_2$-		[58]
Laberty-Robert		Review			[59]
Ladewig	SiO_2		Methyldimethoxysilane	DMFC	[60]
Lavorgna	Siloxane	Sulfonated polystyrene			[61]
Lavorgna	Siloxane		Tetraethoxysilane and a mercaptan functionalized organoalkoxysilane		[62]
Lee	SiO_2		3-mercaptopropyltrimethoxysilane precursor		[63]
Lee	SiO_2				[64]

Lee	Pt	Cation exchange, 3 wt%	3-mercaptopropyltrimethoxysilane precursor		[65]
Li	SiO_2			DMFC	[66]
Lin	Amino-SiO_2			Vanadium redox flow batteries	[67]
Ludvigsson****	Mn_3O_4, $LiCoO_2$				[68]
Matos	TiO_2			DEFC	[69]
Matos	Titanate nanotubes			DEFC	[70]
Matos	TiO_2			DEFC	[71]
Mauritz	SiO_2, TiO_2, aluminum, zirconium, organoalkoxysilanes	Review			[72]
Maurtiz	SiO_2				[73]
Maurtiz	SiO_2		Silicon alkoxides		[74]
Maurtiz	SiO_2, TiO_2, aluminum, zirconium, organoalkoxysilanes	Review			[75]
Millet	Pt				[76]
Mistry	SiOP**			PEM	[77]
Mohammadi	ZrO_2-TiO_2	75 nm in mean size		PEMFC	[78]
Nazir	Waterwheel			PEMFC	[79]

	supramolecules				
Norgaard	SnO_2	XRD, TGA	SnCl2		[80]
Parasuraman	Carbon nanorice			Fluorescence	[81]
Park	Ni			Sensor/Actuators	
Patil	Ag	poly (perfluorosulfonic acid)			[82]
Patil	TiO_2	Durability testing	Titanium isopropoxide	PEMFC	[83]
Patil	TiO_2	Durability Testing	Titanium isopropoxide	PEMFC	[84]
Patil	TiO_2	Durability Testing		PEMFC	[85]
Patil	TiO_2	Quasi networks			[86]
Patra	Ag	Studied different sizes and shapes			[87]
Patra	Ag				[88]
Patra	Ag	Borohydride reuction of a model dye methylene blue.		Catalyst	[89]
Raymond	Fe_2O_3				[90]
Robertson	SiO_2		Tetraethylorthosilicate	PEMFC	[91]
Rodgers	SiO_2			PEMFC	[92]
Shao	SiO_2-TiO_2				[93]
So	SiO_2-P_2O_5		Tetraethoxysilane (TEOS) and trimethylphosphate (TMP)	PEMFC	[94]
Song	Zirconium hydrogen phosphate nanoparticles				[95]
Sun	Ag				[96]
Suresh	PbS				[97]
Teng	TiO_2			Vanadium redox flow	[98]

				batteries	
Teng	SiO_2		Tetraethoxysilane (TEOS) and diethoxydimethylsilane (DEDMS)	Vanadium redox flow batteries	[99]
Teng	SiO_2		Tetraethoxysilane (TEOS)	Vanadium redox flow batteries	[100]
Tripathi		SPEEK-MO_2-PANI (M = Si, Zr and Ti)		DMFC	[101]
Wang	ZnO				[102]
Young	SiO_2		Tetraethoxysilane (TEOS)		[103]
Young	SiO_2		Tetraethoxysilane (TEOS)		[104]
Young	SiO_2	Mechanical testing	Tetraethylorthosilicate and semiorganic silicon alkoxide monomers		[105]
Young	SiO_2		Tetraethylorthosilicate (TEOS) and semiorganic R'Si-n(OR)(4-n) co-monomers		[106]
Yu	SiO_2	Polytetrafluoroethylene (PTFE)	Tetraethoxysilane (TEOS)	PEMFC	[107]
Yu	SiO_2		Tetraethoxysilane (TEOS)	PEMFC	[108]

Table S4: Literature review of works demonstrating the in situ growth of an inorganic phase within Nafion, and to a lesser degree some Nafion related polymers. Search was performed using Web of Knowledge™ utilizing the following search terms: “Nafion ion exchange”, “Nafion ion exchange metal oxide”, “Nafion ion exchange nanoparticle”, “Nafion ion exchange in situ”, “Nafion ion exchange in situ nanoparticle”. “Nafion template”, “Nafion template metal oxide”, “Nafion template nanoparticle”, “Nafion template sol gel”, “Nafion sol gel”, “Nafion sol gel nanoparticle”. Search results yielded 748 candidates (after removing duplicates), of which 102 were deemed relevant. Search was performed on 05/28/2015. Precursors are listed when noted in the abstract.

REFERENCES:

1. *Industrial Applications of X-ray Diffraction*. Marcel Dekker: New York, 2000.
2. Pesika, N. S.; Stebe, K. J.; Searson, P. C., Determination of the particle size distribution of quantum nanocrystals from absorbance spectra. *Advanced Materials* **2003,** *15* (15), 1289-+.
3. (a) Brus, L., ELECTRONIC WAVE-FUNCTIONS IN SEMICONDUCTOR CLUSTERS - EXPERIMENT AND THEORY. *J. Phys. Chem.* **1986,** *90* (12), 2555-2560; (b) Brus, L. E., ELECTRON ELECTRON AND ELECTRON-HOLE INTERACTIONS IN SMALL SEMICONDUCTOR CRYSTALLITES - THE SIZE DEPENDENCE OF THE LOWEST EXCITED ELECTRONIC STATE. *J. Chem. Phys.* **1984,** *80* (9), 4403-4409.
4. Vishnyakov, A.; Neimark, A. V., Self-Assembly in Nafion Membranes upon Hydration: Water Mobility and Adsorption Isotherms. *Angewandte Chemie-International Edition* **2014**.
5. (a) Vishnyakov, A.; Neimark, A. V., Molecular simulation study of Nafion membrane solvation in water and methanol. *Journal of Physical Chemistry B* **2000,** *104* (18), 4471-4478; (b) Vishnyakov, A.; Neimark, A. V., Molecular dynamics simulation of nafion oligomer solvation in equimolar methanol-water mixture. *Journal of Physical Chemistry B* **2001,** *105* (32), 7830-7834; (c) Vishnyakov, A.; Neimark, A. V., Specifics of solvation of sulfonated polyelectrolytes in water, dimethylmethylphosphonate, and their mixture: A molecular simulation study. *Journal of Chemical Physics* **2008,** *128* (16), 164902.
6. Lyubartsev, A. P.; Laaksonen, A., M.DynaMix - a scalable portable parallel MD simulation package for arbitrary molecular mixtures. *Computer Physics Communications* **2000,** *128* (3), 565-589.
7. (a) Hoover, W. G., CANONICAL DYNAMICS - EQUILIBRIUM PHASE-SPACE DISTRIBUTIONS. *Physical Review A* **1985,** *31* (3), 1695-1697; (b) Nose, S., A UNIFIED FORMULATION OF THE CONSTANT TEMPERATURE MOLECULAR-DYNAMICS METHODS. *Journal of Chemical Physics* **1984,** *81* (1), 511-519.
8. Lyubartsev, A. P.; Karttunen, M.; Vattulainen, I.; Laaksonen, A., On coarse-graining by the inverse Monte Carlo method: Dissipative particle dynamics simulations made to a precise tool in soft matter modeling. *Soft Mater.* **2003,** *1* (1), 121-137.
9. Ai, F.; Chen, H.; Zhang, S. H.; Liu, S. Y.; Wei, F.; Dong, X. Y.; Cheng, J. K.; Huang, W. H., Real-Time Monitoring of Oxidative Burst from Single Plant Protoplasts Using Microelectrochemical Sensors Modified by Platinum Nanoparticles. *Anal. Chem.* **2009,** *81* (20), 8453-8458.
10. Alberti, G.; Casciola, M.; Pica, M.; Tarpanelli, T.; Sganappa, M., New preparation methods for composite membranes for medium temperature fuel cells based on precursor solutions of insoluble inorganic compounds. *Fuel Cells* **2005,** *5* (3), 366-374.
11. Amiinu, I. S.; Li, W.; Wang, G. J.; Tu, Z. K.; Tang, H. L.; Pan, M.; Zhang, H. N., Toward Anhydrous Proton Conductivity Based on Imidazole Functionalized Mesoporous Silica/Nafion Composite Membranes. *Electrochim. Acta 160*, 185-194.
12. Amjadi, M.; Rowshanzamir, S.; Peighambardoust, S. J.; Hosseini, M. G.; Eikani, M. H., Investigation of physical properties and cell performance of Nafion/TiO2 nanocomposite membranes for high temperature PEM fuel cells. *Int. J. Hydrog. Energy 35* (17), 9252-9260.
13. Babu, K. S.; Vijayan, C.; Devanathan, R., Strong quantum confinement effects in polymer-based PbS nanostructures prepared by ion-exchange method. *Materials Letters* **2004,** *58* (7-8), 1223-1226.

14. Baradie, B.; Dodelet, J. P.; Guay, D., Hybrid Nafion (R)-inorganic membrane with potential applications for polymer electrolyte fuel cells. *Journal of Electroanalytical Chemistry* **2000,** *489* (1-2), 101-105.
15. Cele, N.; Ray, S. S., Recent Progress on Nafion-Based Nanocomposite Membranes for Fuel Cell Applications. *Macromol. Mater. Eng.* **2009,** *294* (11), 719-738.
16. Chaudhury, S.; Agarwal, C.; Pandey, A. K.; Aher, V. T.; Panicker, L.; Ramagiri, S. V.; Bellare, J. R.; Goswami, A., Counter-ions diffusion properties of silica embedded poly(perfluorosulfonic) acid membrane. *J. Membr. Sci. 382* (1-2), 262-270.
17. Chen, C. Y.; Garnica-Rodriguez, J. I.; Duke, M. C.; Dalla Costa, R. F.; Dicks, A. L.; da Costa, J. C. D., Nafion/polyaniline/silica composite membranes for direct methanol fuel cell application. *J. Power Sources* **2007,** *166* (2), 324-330.
18. Chen, Z. W.; Holmberg, B.; Li, W. Z.; Wang, X.; Deng, W. Q.; Munoz, R.; Yan, Y. S., Nafion/zeolite nanocomposite membrane by in situ crystallization for a direct methanol fuel cell. *Chem. Mat.* **2006,** *18* (24), 5669-5675.
19. Chi, W. S.; Jeon, Y.; Park, S. J.; Kim, J. H.; Shul, Y. G., Fabrication of Surface-Patterned Membranes by Means of a ZnO Nanorod Templating Method for Polymer Electrolyte Membrane Fuel-Cell Applications. *Chempluschem 79* (8), 1109-1115.
20. Choi, E. J.; Kang, C. H.; Choi, H. N.; Lee, W. Y., Electrogene rated Chemiluminescence Sensor Based on Tris(2,2 '-bipyridyl) ruthenium(II) Immobilized in the Composite Film of Multi-walled Carbon Nanotube/Sol-gel Zinc oxide/Nafion. *Bull. Korean Chem. Soc.* **2009,** *30* (10), 2387-2392.
21. Choi, P.; Jalani, N. H.; Datta, R., Thermodynamics and proton transport in Nafion - III. Proton transport in Nafion/sulfated ZrO2 nanocomposite membranes. *Journal of the Electrochemical Society* **2005,** *152* (8), A1548-A1554.
22. Choi, W. C.; Jeon, M. K.; Kim, Y. J.; Woo, S. I.; Hong, W. H., Development of enhanced materials for direct-methanol fuel cell by combinatorial method and nanoscience. *Catal. Today* **2004,** *93-5*, 517-522.
23. Chowdhury, S. R.; ten Elshof, J. E.; Benes, N. E.; Keizer, K., Development and comparative study of different nanofiltration membranes for recovery of highly charged large ions. *Desalination* **2002,** *144* (1-3), 41-46.
24. Colicchio, I.; Wen, F.; Keul, H.; Simon, U.; Moeller, M., Sulfonated poly(ether ether ketone)-silica membranes doped with phosphotungstic acid. Morphology and proton conductivity. *J. Membr. Sci.* **2009,** *326* (1), 45-57.
25. Cui, Z. M.; Xing, W.; Liu, C. P.; Liao, J. H.; Zhang, H., Chitosan/heteropolyacid composite membranes for direct methanol fuel cell. *J. Power Sources* **2009,** *188* (1), 24-29.
26. Daiko, Y.; Klein, L. C.; Kasuga, T.; Nogami, M., Hygroscopic-oxides/Nafion (R) hybrid electrolyte for direct methanol fuel cells. *Journal of Membrane Science* **2006,** *281* (1-2), 619-625.
27. Daiko, Y.; Klein, L. C.; Nogami, M., Modifying Nafion with nanostructured inorganic oxides for proton exchange membrane fuel cells. In *Nanostructured Materials in Alternative Energy Devices*, Kelder, E. M.; Leite, E. R.; Tarascon, J. M.; Chiang, Y. M., Eds. Materials Research Society: Warrendale, 2004; Vol. 822, pp 153-158.
28. Daiko, Y.; Sakamoto, H.; Katagiri, K.; Muto, H.; Sakai, M.; Matsuda, A., Deposition of ultrathin nafion layers on sol-gel-derived phenylsilsesquioxane particles via layer-by-layer assembly. *Journal of the Electrochemical Society* **2008,** *155* (5), B479-B482.

29. Damay, F.; Klein, L. C., Transport properties of Nafion (TM) composite membranes for proton-exchange membranes fuel cells. *Solid State Ionics* **2003,** *162*, 261-267.
30. Deng, Q.; Cable, K. M.; Moore, R. B.; Mauritz, K. A., Small-angle X-ray scattering studies of Nafion(R)/[silicon oxide] and Nafion(R)/ORMOSlL nanocomposites. *Journal of Polymer Science Part B-Polymer Physics* **1996,** *34* (11), 1917-1923.
31. Deng, Q.; Hu, Y.; Moore, R. B.; McCormick, C. L.; Mauritz, K. A., Nafion/ORMOSIL hybrids via in situ sol-gel reactions .3. Pyrene fluorescence probe investigations of nanoscale environment. *Chemistry of Materials* **1997,** *9* (1), 36-44.
32. Deng, Q.; Jarrett, W.; Moore, R. B.; Mauritz, K. A., Novel nafion(R)/ORMOSIL hybrids via ipl situ sol-gel-reactions .2. Probe of ORMOSIL phase nanostructure by Si-29 solid state NMR spectroscopy. *Journal of Sol-Gel Science and Technology* **1996,** *7* (3), 177-190.
33. Deng, Q.; Moore, R. B.; Mauritz, K. A., Novel Nafion ORMOSIL hybrids via in situ sol-gel reactions .1. Probe of ORMOSIL phase nanostructures by infrared spectroscopy. *Chemistry of Materials* **1995,** *7* (12), 2259-2268.
34. Deng, Q.; Moore, R. B.; Mauritz, K. A., Nafion (R) (SiO2, ORMOSIL, and dimethylsiloxane) hybrids via in situ sol-gel reactions: Characterization of fundamental properties. *Journal of Applied Polymer Science* **1998,** *68* (5), 747-763.
35. Deng, Q.; Wilkie, C. A.; Moore, R. B.; Mauritz, K. A., TGA-FTi.r. investigation of the thermal degradation of Nafion (R) and Nafion (R)/[silicon oxide]-based nanocomposites. *Polymer* **1998,** *39* (24), 5961-5972.
36. Doyle, R. L.; Lyons, M. E. G., Redox and Oxygen Evolution Electrocatalytic Properties of Nafion and Single-Walled Carbon Nanotube/Hydrous Iron Oxide Composite Films. *Electrocatalysis 5* (2), 114-124.
37. Dresch, M. A.; Matos, B. R.; Fonseca, F. C.; Santiago, E. I.; Carmo, M.; Lanfredi, A. J. C.; Balog, S., Small-angle X-ray and neutron scattering study of Nafion-SiO2 hybrid membranes prepared in different solvent media. *Journal of Power Sources 274*, 560-567.
38. Dupuis, A.-C., Proton exchange membranes for fuel cells operated at medium temperatures: Materials and experimental techniques. *Progress in Materials Science 56* (3), 289-327.
39. Hill, M. L.; Kim, Y. S.; Einsla, B. R.; McGrath, J. E., Zirconium hydrogen phosphate/disulfonated poly(arylene ether sulfone) copolymer composite membranes for proton exchange membrane fuel cells. *Journal of Membrane Science* **2006,** *283* (1-2), 102-108.
40. Huang, J.-F., Cu+ assisted preparation of mesoporous Pt-organic composites for highly selective and sensitive non-enzymatic glucose sensing. *Journal of Materials Chemistry B 2* (10), 1354-1361.
41. Ingle, N. J. C.; Sode, A.; Martens, I.; Gyenge, E.; Wilkinson, D. P.; Bizzotto, D., Synthesis and Characterization of Diverse Pt Nanostructures in Nafion. *Langmuir 30* (7), 1871-1879.
42. Jalani, N. H.; Dunn, K.; Datta, R., Synthesis and characterization of Nafion (R)-MO2 (M = Zr, Si, Ti) nanocomposite membranes for higher temperature PEM fuel cells. *Electrochimica Acta* **2005,** *51* (3), 553-560.
43. Jiang, R. C.; Kunz, H. R.; Fenton, J. M., Composite silica/Nafion (R) membranes prepared by tetraethylorthosilicate sol-gel reaction and solution casting for direct methanol fuel cells. *Journal of Membrane Science* **2006,** *272* (1-2), 116-124.

44. Jian-hua, T.; Peng-fei, G.; Zhi-yuan, Z.; Wen-hui, L.; Zhony-qiang, S., Preparation and performance evaluation of a Nafion-TiO2 composite membrane for PEMFCs. *International Journal of Hydrogen Energy* **2008,** *33* (20), 5686-5690.
45. Jung, D. H.; Cho, S. Y.; Peck, D. H.; Shin, D. R.; Kim, J. S., Performance evaluation of a Nafion/silicon oxide hybrid membrane for direct methanol fuel cell. *Journal of Power Sources* **2002,** *106* (1-2), 173-177.
46. Kang, S.; Peck, D. H.; Park, Y. C.; Jung, D. H.; Jang, J. H.; Lee, H. R., Hydroscopic strontium hydroxide/Nafion composite membrane for a direct methanol fuel cell. *Journal of Physics and Chemistry of Solids* **2008,** *69* (5-6), 1280-1283.
47. Ke, C. C.; Li, X. J.; Qu, S. G.; Shao, Z. G.; Yi, B. L., Preparation and properties of Nafion/SiO2 composite membrane derived via in situ sol-gel reaction: size controlling and size effects of SiO2 nano-particles. *Polym. Adv. Technol. 23* (1), 92-98.
48. Ke, C.-C.; Li, X.-J.; Shen, Q.; Qu, S.-G.; Shao, Z.-G.; Yi, B.-L., Investigation on sulfuric acid sulfonation of in-situ sol-gel derived Nafion/SiO2 composite membrane. *International Journal of Hydrogen Energy 36* (5), 3606-3613.
49. Kim, B. H.; Park, S. B.; Oh, M.-H.; Park, Y.-i., Fluoroalkylsilane/Nafion (R) Composite Electrolyte Membranes. *Journal of the Korean Physical Society 59* (4), 2811-2816.
50. Kim, H. S.; Han, J. W.; Chun, K. Y.; Shul, Y. G.; Joe, Y. I., SYNTHESIS OF ORGANIC-INORGANIC COMPOSITE MEMBRANE BY SOL-GEL PROCESS. *Korean Journal of Chemical Engineering* **1995,** *12* (4), 405-409.
51. Kim, S. J.; Kim, H. M.; Yoo, Y. T.; Haw, J. R.; Kim, S. G.; Jang, M. H.; Lim, S. K., X+-beta "-aluminas/Naflon (X = H3O, NH4) hybrid membranes for high-temperature PEMFCs. *J. Ceram. Process. Res.* **2009,** *10* (2), 176-182.
52. Kim, Y. J.; Choi, W. C.; Woo, S. I.; Hong, W. H., Evaluation of a palladinized Nafion (TM) for direct methanol fuel cell application. *Electrochimica Acta* **2004,** *49* (19), 3227-3234.
53. Kim, Y. J.; Choi, W. C.; Woo, S. I.; Hong, W. H., Proton conductivity and methanol permeation in Nafion((TM))/ORMOSIL prepared with various organic silanes. *J. Membr. Sci.* **2004,** *238* (1-2), 213-222.
54. Klein, L. C., Sol-Gel Process for Proton Exchange Membranes. In *Progress in Sol-Gel Production*, Esquivias, L., Ed. Trans Tech Publications Ltd: Stafa-Zurich, 2009; Vol. 391, pp 159-168.
55. Korin, E.; Siton, O.; Bettelheim, A., Fuel cells and ionically conductive membranes: An overview. *Reviews in Chemical Engineering* **2007,** *23* (1), 35-63.
56. Kumar, R.; Pandey, A. K.; Dhara, S.; Misra, N. L.; Ramagiri, S. V.; Bellare, J. R.; Goswami, A., Inclusion of silver nanoparticles in host poly(perfluorosulfonic) acid membrane using ionic and non-ionic reductants. *Journal of Membrane Science 352* (1-2), 247-254.
57. Kumar, R.; Pandey, A. K.; Sharma, M. K.; Panicker, L. V.; Sodaye, S.; Suresh, G.; Ramagiri, S. V.; Bellare, J. R.; Goswami, A., Diffusional Transport of Ions in Plasticized Anion-Exchange Membranes. *J. Phys. Chem. B 115* (19), 5856-5867.
58. Kumar, R.; Pandey, A. K.; Tyagi, A. K.; Dey, G. K.; Ramagiri, S. V.; Bellare, J. R.; Goswami, A., In situ formation of stable gold nanoparticles in polymer inclusion membranes. *Journal of Colloid and Interface Science* **2009,** *337* (2), 523-530.
59. Laberty-Robert, C.; Valle, K.; Pereira, F.; Sanchez, C., Design and properties of functional hybrid organic-inorganic membranes for fuel cells. *Chemical Society Reviews 40* (2), 961-1005.

60. Ladewig, B. P.; Knott, R. B.; Martin, D. J.; da Costa, J. C. D.; Lu, G. Q., Nafion-MPMDMS nanocomposite membranes with low methanol permeability. *Electrochemistry Communications* **2007,** *9* (4), 781-786.
61. Lavorgna, M.; Fusco, L.; Piscitelli, F.; Mensitieri, G.; Agoretti, P.; Borriello, A.; Mascia, L., Control of Morphology of Sulfonated Syndio-Polystyrene Membranes Through Constraints Imposed by Siloxane Networks. *Polymer Engineering and Science* **2008,** *48* (12), 2389-2399.
62. Lavorgna, M.; Mascia, L.; Mensitieri, G.; Gilbert, M.; Scherillo, G.; Palomba, B., Hybridization of Nafion membranes by the infusion of functionalized siloxane precursors. *J. Membr. Sci.* **2007,** *294* (1-2), 159-168.
63. Lee, H.; Park, S. B.; Oh, M.-H.; Coo, K.; Park, Y.-i.; Suzuki, S.; Nagai, M.; Prinz, F. B., Modification of Nafion (R) Using 3-mercaptopropyl Trimethoxysilane. *Journal of the Korean Physical Society 56* (4), 1215-1222.
64. Lee, H.; Park, S. B.; Oh, M.-H.; Kim, S.; Hwang, H. J.; Lee, H.-K.; Park, Y.-i., Properties of modified NafionA (R) membranes with heavy amount of (3-mercaptopropyl) trimethoxysilane prepared by long-term infiltration. *Metals and Materials International 16* (3), 477-481.
65. Lee, P.-C.; Han, T.-H.; Kim, D. O.; Lee, J.-H.; Kang, S.-J.; Chung, C.-H.; Lee, Y.; Cho, S. M.; Choi, H.-G.; Kim, T.; Lee, E.; Nam, J.-D., In situ formation of platinum nanoparticles in Nafion recast film for catalyst-incorporated ion-exchange membrane in fuel cell applications. *Journal of Membrane Science* **2008,** *322* (2), 441-445.
66. Li, T.; Yang, Y., A novel inorganic/organic composite membrane tailored by various organic silane coupling agents for use in direct methanol fuel cells. *Journal of Power Sources* **2009,** *187* (2), 332-340.
67. Lin, C.-H.; Yang, M.-C.; Wei, H.-J., Amino-silica modified Nafion membrane for vanadium redox flow battery. *Journal of Power Sources 282*, 562-571.
68. Ludvigsson, M.; Lindgren, J.; Tegenfeldt, R., Incorporation and characterisation of oxides of manganese, cobalt and lithium into Nafion 117 membranes. *Journal of Materials Chemistry* **2001,** *11* (4), 1269-1276.
69. Matos, B. R.; Isidoro, R. A.; Santiago, E. I.; Fonseca, F. C., Performance enhancement of direct ethanol fuel cell using Nafion composites with high volume fraction of titania. *Journal of Power Sources 268*, 706-711.
70. Matos, B. R.; Isidoro, R. A.; Santiago, E. I.; Linardi, M.; Ferlauto, A. S.; Tavares, A. C.; Fonseca, F. C., In Situ Fabrication of Nafion-Titanate Hybrid Electrolytes for High-Temperature Direct Ethanol Fuel Cell. *Journal of Physical Chemistry C 117* (33), 16863-16870.
71. Matos, B. R.; Isidoro, R. A.; Santiago, E. I.; Tavares, A. C.; Ferlauto, A. S.; Muccillo, R.; Fonseca, F. C., Nafion-titanate nanotubes composites prepared by in situ crystallization and casting for direct ethanol fuel cells. *International Journal of Hydrogen Energy 40* (4), 1859-1867.
72. Mauritz, K. A., Organic-inorganic hybrid materials: perfluorinated ionomers as sol-gel polymerization templates for inorganic alkoxides. *Mater. Sci. Eng. C-Biomimetic Supramol. Syst.* **1998,** *6* (2-3), 121-133.
73. Mauritz, K. A.; Hassan, M. K., Nanophase separated perfluorinated ionomers as sol-gel polymerization templates for functional inorganic oxide nanoparticles. *Polymer Reviews* **2007,** *47* (4), 543-565.
74. Mauritz, K. A.; Mountz, D. A.; Reuschle, D. A.; Blackwell, R. I., Self-assembled organic/inorganic hybrids as membrane materials. *Electrochimica Acta* **2004,** *50* (2-3), 565-569.

75. Mauritz, K. A.; Payne, J. T., [Perfluorosulfonate ionomer]/silicate hybrid membranes via base-catalyzed in situ sol-gel processes for tetraethylorthosilicate. *Journal of Membrane Science* **2000,** *168* (1-2), 39-51.
76. Millet, P.; Durand, R.; Dartyge, E.; Tourillon, G.; Fontaine, A., PRECIPITATION OF METALLIC PLATINUM INTO NAFION IONOMER MEMBRANES .1. EXPERIMENTAL RESULTS. *Journal of the Electrochemical Society* **1993,** *140* (5), 1373-1380.
77. Mistry, M. K.; Choudhury, N. R.; Dutta, N. K.; Knott, R.; Shi, Z.; Holdcroft, S., Novel Organic-Inorganic Hybrids with Increased Water Retention for Elevated Temperature Proton Exchange Membrane Application. *Chemistry of Materials* **2008,** *20* (21), 6857-6870.
78. Mohammadi, G.; Jahanshahi, M.; Rahimpour, A., Fabrication and evaluation of Nafion nanocomposite membrane based on ZrO2-TiO2 binary nanoparticles as fuel cell MEA. *International Journal of Hydrogen Energy 38* (22), 9387-9394.
79. Nazir, N. A.; Kudo, H.; Nishikubo, T.; Kyu, T., Impregnation of waterwheel supramolecules as proton carriers in Nafion-perfluorinated ionomer membranes. *Journal of Materials Science 47* (20), 7269-7279.
80. Norgaard, C. F.; Nielsen, U. G.; Skou, E. M., Preparation of Nafion 117 (TM)-SnO2 composite membranes using an ion-exchange method. *Solid State Ionics 213*, 76-82.
81. Parasuraman, P. S.; Tsai, H. C.; Imae, T., In-situ hydrothermal synthesis of carbon nanorice using Nafion as a template. *Carbon 77*, 660-666.
82. Patil, P. N.; Sudarshan, K.; Sharma, S. K.; Dutta, D.; Maheshwari, P.; Pujari, P. K., Microstructural studies of poly (perfluorosulfonic acid) membrane doped with silver nanoparticles using positron annihilation spectroscopy. In *12th International Workshop on Slow Positron Beam Techniques*, Buckman, S. J.; Sullivan, J. P.; Makochekanwa, C.; White, R., Eds. Vol. 262.
83. Patil, Y.; Kulkarni, S.; Mauritz, K. A., In Situ Grown Titania Composition for Optimal Performance and Durability of Nafion (R) Fuel Cell Membranes. *Journal of Applied Polymer Science 121* (4), 2344-2353.
84. Patil, Y.; Mauritz, K. A., Durability Enhancement of Nafion (R) Fuel Cell Membranes Via In Situ Sol-Gel-Derived Titanium Dioxide Reinforcement. *Journal of Applied Polymer Science* **2009,** *113* (5), 3269-3278.
85. Patil, Y.; Sambandam, S.; Ramani, V.; Mauritz, K., Perfluorinated Polymer Electrolytes Hybridized with In situ Grown Titania Quasi-Networks. *Acs Applied Materials & Interfaces 5* (1), 42-48.
86. Patil, Y.; Sambandam, S.; Ramani, V.; Mauritz, K., Model Studies of the Durability of a Titania-Modified Nafion Fuel Cell Membrane. *Journal of the Electrochemical Society* **2009,** *156* (9), B1092-B1098.
87. Patra, S.; Pandey, A. K.; Sen, D.; Ramagiri, S. V.; Bellare, J. R.; Mazumder, S.; Goswami, A., Redox Decomposition of Silver Citrate Complex in Nanoscale Confinement: An Unusual Mechanism of Formation and Growth of Silver Nanoparticles. *Langmuir 30* (9), 2460-2469.
88. Patra, S.; Sen, D.; Pandey, A. K.; Agarwal, C.; Ramagiri, S. V.; Bellare, J. R.; Mazumder, S.; Goswami, A., Local Conditions Influencing In Situ Formation of Different Shaped Silver Nanostructures and Subsequent Reorganizations in Ionomer Membrane. *Journal of Physical Chemistry C 117* (23), 12026-12037.

89. Patra, S.; Sen, D.; Pandey, A. K.; Bahadur, J.; Mazumder, S.; Ramagiri, S. V.; Bellare, J. R.; Roth, S. V.; Santoro, G.; Yu, S.; Goswami, A., Time resolved growth of membrane stabilized silver NPs and their catalytic activity. *RSC Adv. 4* (103), 59379-59386.
90. Raymond, L.; Revol, J. F.; Ryan, D. H.; Marchessault, R. H., Precipitation of ferrites in Nafion(R) membranes. *Journal of Applied Polymer Science* **1996,** *59* (7), 1073-1086.
91. Robertson, M. A. F.; Mauritz, K. A., Infrared investigation of the silicon oxide phase in [perfluoro-carboxylate/sulfonate (bilayer)]/[silicon oxide] nanocomposite membranes. *Journal of Polymer Science Part B-Polymer Physics* **1998,** *36* (4), 595-606.
92. Rodgers, M. P.; Shi, Z. Q.; Holdcroft, S., Transport properties of composite membranes containing silicon dioxide and Nafion (R). *J. Membr. Sci.* **2008,** *325* (1), 346-356.
93. Shao, P. L.; Mauritz, K. A.; Moore, R. B., [Perfluorosulfonate ionomer] [SiO2-TiO2] nanocomposites via polymer-in situ sol-gel chemistry: Sequential alkoxide procedure. *Journal of Polymer Science Part B-Polymer Physics* **1996,** *34* (5), 873-882.
94. So, S. Y.; Kim, S. C.; Lee, S.-Y., In situ hybrid Nafion/SiO2-P2O5 proton conductors for high-temperature and low-humidity proton exchange membrane fuel cells. *Journal of Membrane Science 360* (1-2), 210-216.
95. Song, M. K.; Hwang, J. S.; Kim, Y. T.; Rhee, H. W.; Kim, J., Characterization of nanostructured organic-inorganic hybrid membranes. *Molecular Crystals and Liquid Crystals* **2003,** *407*, 421-428.
96. Sun, Y. P.; Atorngitjawat, P.; Lin, Y.; Liu, P.; Pathak, P.; Bandara, J.; Elgin, D.; Zhang, M. Z., Nanoscale cavities in ionomer membrane for the formation of nanoparticles. *J. Membr. Sci.* **2004,** *245* (1-2), 211-217.
97. Suresh Babu, K.; Vijayan, C.; Haridoss, P., Properties of size-tuned PbS nanocrystals stabilized in a polymer template. *Materials Research Bulletin* **2007,** *42* (6), 996-1003.
98. Teng, X.; Zhao, Y.; Xi, J.; Wu, Z.; Qiu, X.; Chen, L., Nafion/organic silica modified TiO2 composite membrane for vanadium redox flow battery via in situ sol-gel reactions. *Journal of Membrane Science* **2009,** *341* (1-2), 149-154.
99. Teng, X.; Zhao, Y.; Xi, J.; Wu, Z.; Qiu, X.; Chen, L., Nafion/organically modified silicate hybrids membrane for vanadium redox flow battery. *Journal of Power Sources* **2009,** *189* (2), 1240-1246.
100. Teng, X. G.; Dai, J. C.; Bi, F. Y.; Yin, G. P., Ultra-thin polytetrafluoroethene/Nafion/silica composite membrane with high performance for vanadium redox flow battery. *J. Power Sources 272*, 113-120.
101. Tripathi, B. P.; Shahi, V. K., Surface redox polymerized SPEEK-MO2-PANI (M = Si, Zr and Ti) composite polyelectrolyte membranes impervious to methanol. *Colloids and Surfaces a-Physicochemical and Engineering Aspects* **2009,** *340* (1-3), 10-19.
102. (a) Wang, H.; Liu, P.; Wang, S.; Han, W.; Wang, X.; Fu, X., Nanocrystalline zinc oxide in perfluorinated ionomer membranes: Preparation, characterization, and photocatalytic properties. *Journal of Molecular Catalysis a-Chemical* **2007,** *273* (1-2), 21-25; (b) Wang, J.; Liu, P.; Fu, X.; Li, Z.; Han, W.; Wang, X., Relationship between Oxygen Defects and the Photocatalytic Property of ZnO Nanocrystals in Nafion Membranes. *Langmuir* **2009,** *25* (2), 1218-1223.
103. Young, S. K.; Jarrett, W. L.; Mauritz, K. A., Studies of the aging of Nafion (R)/silicate nanocomposites using Si-29 solid state NMR spectroscopy. *Polymer Engineering and Science* **2001,** *41* (9), 1529-1539.

104. Young, S. K.; Jarrett, W. L.; Mauritz, K. A., Nafion (R)/ORMOSIL nanocomposites via polymer-in situ sol-gel reactions. 1. Probe of ORMOSIL phase nanostructures by Si-29 solid-state NMR spectroscopy. *Polymer* **2002,** *43* (8), 2311-2320.
105. Young, S. K.; Mauritz, K. A., Dynamic mechanical analyses of Nafion (R)/organically modified silicate nanocomposites. *Journal of Polymer Science Part B-Polymer Physics* **2001,** *39* (12), 1282-1295.
106. Young, S. K.; Mauritz, K. A., Nafion (R)/(organically modified silicate) nanocomposites via polymer in situ sol-gel reactions: Mechanical tensile properties. *Journal of Polymer Science Part B-Polymer Physics* **2002,** *40* (19), 2237-2247.
107. Yu, H.; Shi, J.; Zeng, X.; Bao, M.; Zhao, X., A proton-exchange membrane prepared by the radiation grafting of styrene and silica into polytetrafluoroethylene films. *Radiation Physics and Chemistry* **2009,** *78* (7-8), 497-500.
108. Yu, J.; Pan, M.; Yuan, R. Z., Nafion/silicon oxide composite membrane for high temperature proton exchange membrane fuel cell. *Journal of Wuhan University of Technology-Materials Science Edition* **2007,** *22* (3), 478-481.